A measurement of noise created by fluctuating electrostatic charges on dielectric surfaces using a torsion balance

P Campsie, J Hough, S Rowan and G D Hammond†

SUPA‡ Institute for Gravitational Research, School of Physics and Astronomy, University of Glasgow, Glasgow, G12 8QQ, UK

E-mail: `Giles.Hammond@glasgow.ac.uk`

Abstract. Future gravitational wave detectors could have their sensitivity significantly limited, at frequencies below 10 Hz, by the presence of fluctuating electrostatic charges on the dielectric surfaces of the detector optics. A confirmed observation of the effect of fluctuating charges, or charging noise, in a gravitational wave detector has still to be made and it has never been experimentally verified by any other means. This paper presents a direct measurement of the fluctuating force noise created by moving charges on a dielectric surface using a servo controlled torsion balance. The results confirm that the fluctuating force noise caused by excess charges can be best described by a Markov process with a single correlation time and has a frequency dependence of f^{-1}.

PACS numbers: 07.10.Pz 73.40.-c 05.40.-a 04.80.Nn 07.30.-t 95.55.Ym 07.60.Ly

Submitted to: *Class. Quantum Grav.*

† corresponding author
‡ Scottish Universities Physics Alliance

1. Introduction

A world wide network of long base-line interferometric detectors are currently used to attempt to detect propagating tidal variations in space-time, known as gravitational waves, caused by astrophysical events. The first generation network consisted of six detectors: three that formed the LIGO network [1], the French/Italian Virgo detector [2], the British/German GEO600 detector [3] and the Japanese TAMA300 detector [4]. In order to improve the chances of detection these instruments are undergoing upgrades, or have already been upgraded, to an advanced detector status, with the exception of TAMA300. The upgraded LIGO detectors (advanced LIGO) [5] will see their sensitivity increase by a factor of 10 at 150 Hz [6].

A significant amount of the current research into innovative new technologies and materials in the gravitational wave community is focussed on suppressing the limiting noise sources of these complex instruments in order to maximise the chances of detection and maximise the scientific return. However, as the sensitivity of these detectors increases, they will become more susceptible to a particular form of instrument noise which arises due to excess electrostatic charges creating fluctuating Coulomb forces which act on the detector optics. Excess static charges on the detector test masses and suspensions could compromise the sensitivity and control of the detector and may potentially become a limiting noise source in future detectors. Charging noise is thought to have already been observed in one of the initial LIGO detectors [7] and problems due to charging have been encountered at GEO600 relating to the control and positioning of the detector test masses with electrostatic drives [8].

Charging of the test masses can occur through various processes [9]; for example, abrasion with air particles as the vacuum chamber is pumped out, contact with nearby structures such as earthquake stops, during cleaning of the test masses and via cosmic rays hitting the vacuum chamber walls and showering the test masses in electrons [10, 11, 12]. This excess charge creates stray electric fields which act on the optic. These fields fluctuate due to thermally driven processes, such as charge diffusion, which gives rise to a fluctuating force which acts on the test mass. It has been postulated by Weiss [13] that if this fluctuating force, F, decays exponentially across the surface of the optic and is treated as a Markov process with a single

correlation time, τ_0, it will have the form,

$$F = \langle F_0 \rangle \exp\left(-\frac{t}{\tau_0}\right) \tag{1}$$

where $\langle F_0 \rangle$ is the average of the Coulomb force and t is time. Converting (1) to the frequency domain shows that the fluctuating force acting on the optic will produce a power spectrum of the form,

$$F^2(f) = \frac{\langle F_0^2 \rangle}{2\pi\tau_0\left(\frac{1}{\tau_0^2} + (2\pi f)^2\right)} \tag{2}$$

where f is the frequency.

A torsion balance apparatus has been constructed at the University of Glasgow for the purpose of measuring charging noise. A description of the experimental setup, calibration process and the final results will be given in this article.

2. Experimental Setup

The torsion balance consists of an aluminium torsion bob, shown in Figure 1, suspended by a tungsten fibre which has a diameter of 40 μm and a length of 0.6 m. In order to remove the natural stress in the fibre, it was loaded and left to naturally unwind for several weeks before any measurements were made. The bob is suspended from a structure housed completely within a vacuum chamber which can achieve pressures of less than 5×10^{-5} Torr. When left to freely oscillate about its rotational axis defined by the bob's suspending fibre, the bob has a natural period of 178.6 s or 5.6 mHz.

The position of the bob can be adjusted using two Thorlabs PT1/M translation stages, in an x-y configuration, and a Thorlabs CR1/M continuous rotation stage at the suspension point of the fibre. The translation stages allow a 25 mm range of motion and the rotation stage can be continuously rotated. The translation stages allow the bob to be moved in the x and y directions of the x-y plane shown in Figure 1 and the rotation stage allows the rotational position of the bob in the x-y plane to be altered. The rotation stage can be remotely controlled using a stepper motor whilst under vacuum. The stepper motor is connected to a gear box, in order to obtain a finer resolution of the rotational position of the torsion bob, which is attached to the rotation stage's adjusting arm via a universal joint. The stepper motor is controlled using a Saia-Burgess Samotronic 101 stepper motor driver which is connected to a

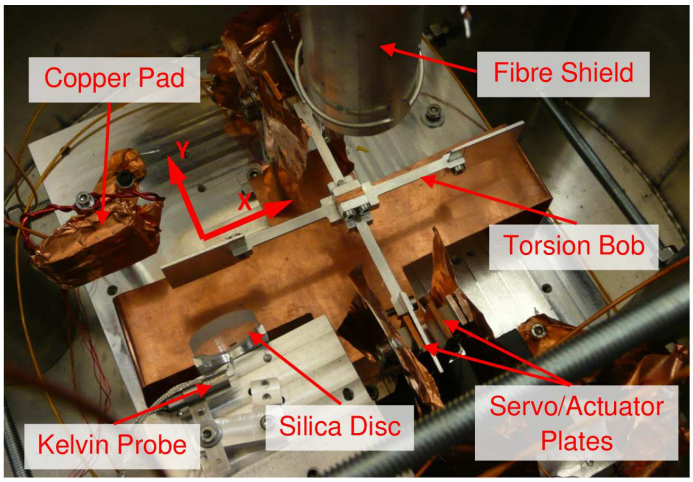

Figure 1. A photograph of the inside of the vacuum chamber where the torsion balance is housed. Stages at the suspension point of the fibre are used to control the bob position in the x-y plane labelled on the photograph. Translation stages allow control of the bob in the x and y directions and a rotation stage allows control of the rotation of the bob in the x-y plane.

PC through a peripheral component interconnect (PCI) 6229 ADC so that it can be programmed using LabVIEW. Each step of the stepper motor results in a 13.1 μrad rotation of the stage and, therefore, a 13.1 μrad rotation of the bob. A diagram of the stepper motor setup can be seen Figure 2.

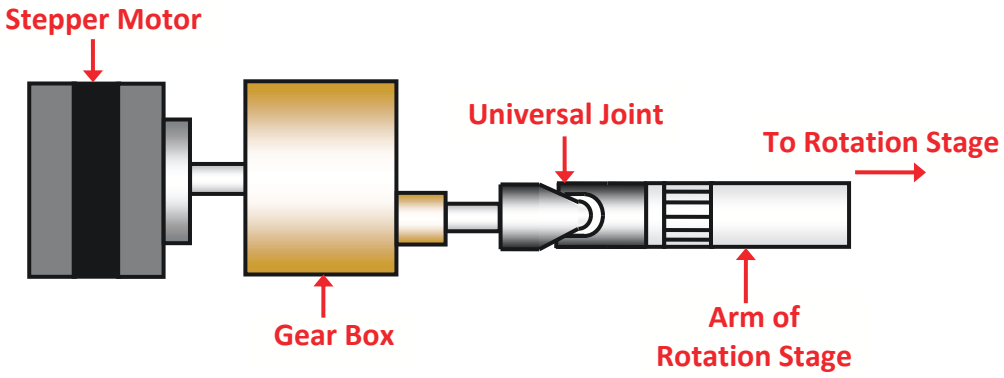

Figure 2. A diagram of the stepper motor setup.

There is a fixed platform near the bottom of the chamber onto which two Thorlabs MTS50-Z8E motorised translation stages, in an x-y configuration, are attached. The motorised translation stages are used to position a one inch silica disc near the bob of the torsion balance in order to make a measurement. Both of these stages have a range of 50 mm. To charge the sample, a large rectangular rubber pad was made from a Viton o-ring and then covered with a thin sheet of copper. This was attached to the fixed platform, near the bottom of the vacuum chamber, using an aluminium post and was positioned near the bob. The copper was electrically isolated from the grounded platform and connected to an electrical feedthrough so that voltages could be applied. This also allowed the pad to be easily grounded during measurements preventing unwanted excess noise. The sample was charged in vacuum by pressing it against the pad using the motorised stages while the pad was held at some potential. Once the charged disc is moved towards the arm of the torsion bob, the electrostatic force of the charge will cause the bob to rotate about the axis defined by its suspending fibre. The copper pad can be seen in Figure 1 and Figure 3.

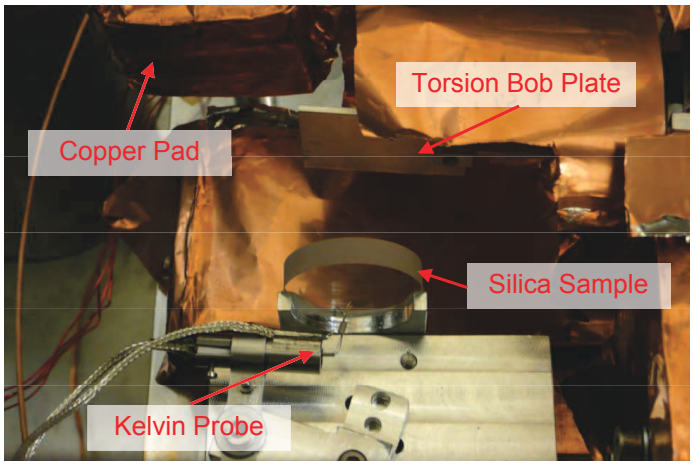

Figure 3. A photograph of the silica sample positioned near the torsion bob to make a measurement of charging noise. The decaying surface charge on the silica disc, which is monitored with the Kelvin probe, exerts a decaying torque on the bob plate. The disc was charged by pressing it against the copper pad whilst the pad had a voltage applied to it.

Also attached to the fixed platform are two columns. Each column has two

copper plates attached to it that sandwich one of the plates on the ends of the arms on the torsion bob (see Figure 1). One copper plate is used for capacitively sensing the rotational position of the bob and the other copper plate is used to apply electrostatic PID (Proportional-Integral-Derivative) servo actuation. The servo actuation is used to counteract the electrostatic force of the charge on the silica disc so that the bob maintains its rotational position during the measurement. The AC sensing signal for the capacitive sensor is applied down the tungsten suspending fibre using a Stanford SR830 lock-in amplifier. This voltage signal has an amplitude of 1 V and a frequency of 100 kHz, which is much greater than the resonant torsional frequency of the bob.

A Besocke Delta Phi Kelvin probe, shown in Figure 1 and Figure 3, was used to monitor the decay of the surface charge on the silica disc sample. From this measurement it is possible to calculate τ_0 from an exponential fit to the decaying signal. The charged face of the silica disc had to be facing the bob, therefore, it was not possible to directly measure this surface charge density. Instead, the Kelvin probe was positioned at the opposite face of the silica disc. This meant that the probe was measuring a polarisation charge induced in the opposite face. This does not affect the outcome of the results as the surface charge and the polarisation charge should decay at the same rate, and the absolute value of the surface charge on the sample is not needed since the Coulomb torque, needed to calculate the torque noise due to charging, can be calculated from the restoring torque of the fibre and the applied servo torque.

More details of the experimental setup, such as the capacitive sensor, PID servo controller and Kelvin probe work, are described in previous publications [14, 15, 16].

3. Calibration

For this experiment it was essential that servo control be used to keep the bob of the torsion balance at a fixed set-point due to the large DC Coulomb force exerted on it by the surface charge. The DC Coulomb force introduces a large negative stiffness to the setup which causes instability. Calibrating the torsion balance while under servo control requires knowledge of the gains of the PID controller, G, the capacitance gradients between the bob and each of the servo plates, $\mathrm{d}C/\mathrm{d}\theta$, and the response function of the torsion bob, T. Transfer functions T and G can be defined in the

Laplace domain as

$$T = \frac{1}{Is^2 + bs + \kappa} \tag{3}$$

and

$$G = \alpha + \frac{\beta}{s} + \gamma s \tag{4}$$

where I is the moment of inertia of the bob, b is the damping constant, κ is the stiffness of the torsion fibre and α, β and γ are the gains of the P, I and D controls respectively. $\mathrm{d}C/\mathrm{d}\theta$ is $(1.2 \pm 0.4) \times 10^{-11}\,\mathrm{F/rad}$ from measurements made in ref. [15]. A schematic of the gains that are taken into consideration in the torsion balance servo control loop is shown in Figure 4.

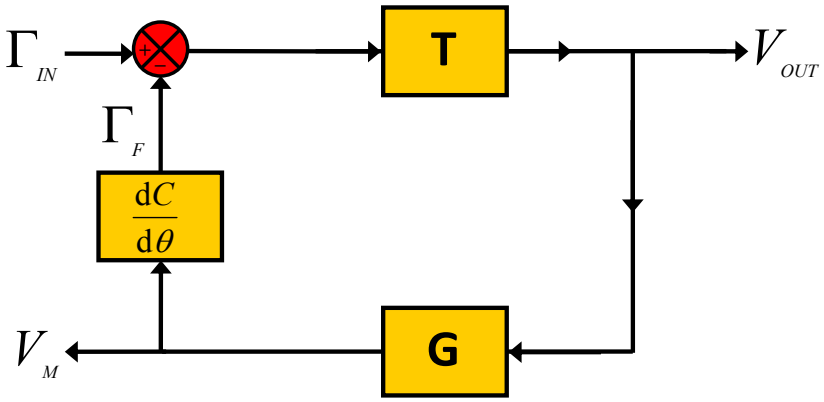

Figure 4. A schematic of the gains that have to be taken into account in the torsion balance setup. A torque acting on the bob, Γ_{IN}, will cause it to rotate and V_{OUT} will be measured by the capacitive sensor. V_{OUT} is also used to calculate the servo voltage, V_M. V_M applies a negative feedback torque, Γ_F, to the bob to counteract its motion and keep it at its set-point.

Using control system theory, an expression can be found that relates the measured servo voltage, V_M, to the torque acting on the bob, Γ_{IN}

$$V_M = \frac{GT}{(1 + GT\,(\mathrm{d}C/\mathrm{d}\theta))}\Gamma_{IN} \tag{5}$$

where $GT/\,(1 + GT\,(\mathrm{d}C/\mathrm{d}\theta))$ is the closed loop gain of the system. Measuring the closed loop gain allows the measured servo voltages to be converted into a torque. To

do this, the stepper motor that controls the rotation stage was programmed to move in a sine wave motion with an amplitude of 100 steps, or 1310 μrad. This causes the bob to oscillate in its rotational plane (the x-y plane labelled in Figure 1). When the torsion bob oscillates in this manner the servo voltages will also oscillate as they try and apply enough feedback torque to keep the bob at its set-point. Γ_{IN} can be calculated from the amplitude of the rotation and the stiffness of the fibre, and the amplitude of V_M is taken as the average peak value of the servo voltage signal. A plot of the stepper motor motion and the servo effort is shown in Figure 5. In this plot the stepper motor was causing the bob to oscillate at a frequency of 0.5 mHz. The peaks and troughs of the servo voltage signal are slightly flattened because of the chosen PID values. Since the PID values had to be much higher than under optimum conditions to control the bob, a saturation effect was observed. It should be noted that this was not saturation of the applied servo voltage.

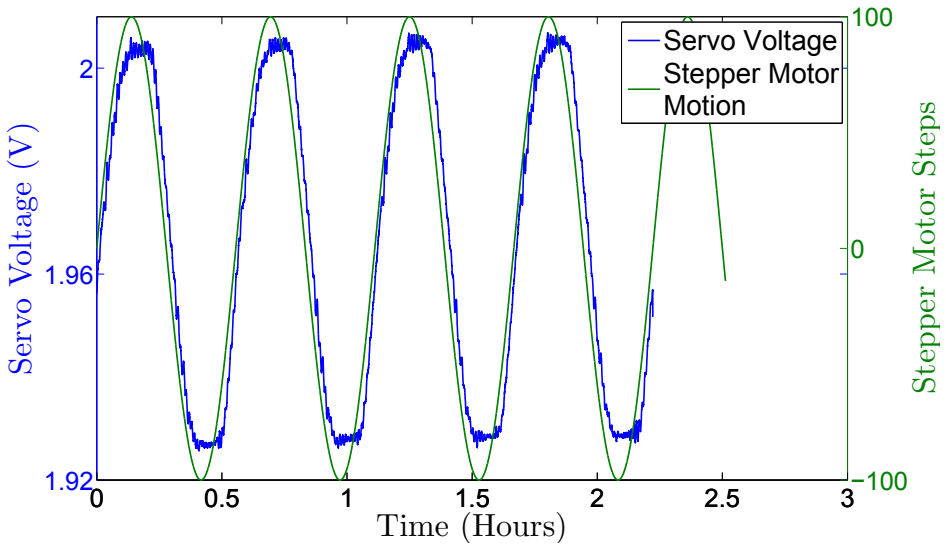

Figure 5. A plot showing the change in servo voltage, blue, and the torsion bob sine wave motion, green, during a measurement of the closed loop gain of the torsion balance system.

The gain which converts the servo voltage into a known torque is calculated simply by dividing the amplitude of Γ_{IN} by the amplitude of V_M. This measurement was carried out for the frequency range 0.25 to 2 mHz and the results are shown in

Figure 6. Measurements were not taken below 0.25 mHz because it would have taken too long and measurements were not taken above 2 mHz because there would not have been enough time to remove backlash as the stepper motor changed direction.

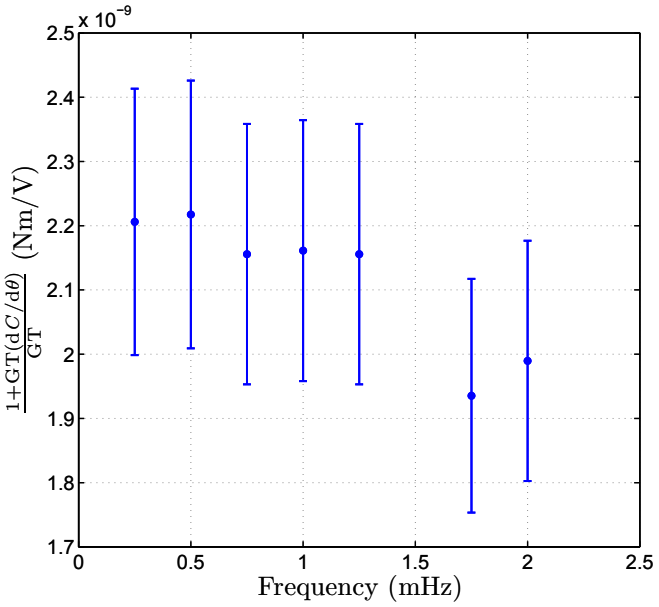

Figure 6. A plot of the inverse of the closed loop gain of the torsion balance system measured at different frequencies.

It is unknown whether the gain measurements at 1.75 mHz and 2 mHz are dropping off as the frequency increases or if they fall within the expected standard deviation of the measurement. Therefore, the data that will be analysed will be below 1.5 mHz because the data definitely appear to level off at these frequencies. The average of the data points below 1.5 mHz is 2.18×10^{-9} Nm/V.

Figure 7 shows a comparison between the instrument noise while the torsion balance is in free running mode (i.e stationary servo voltages) and while the instrument is running under servo control. The two noise plots compare well indicating that the calibration procedure is accurate. It is estimated that the error on the calibration is 9.4% as this was the standard error of the average peak voltage of the servo voltage measured during the calibration. The standard error of the mean is taken as the standard deviation of the sample mean's estimate of the population mean.

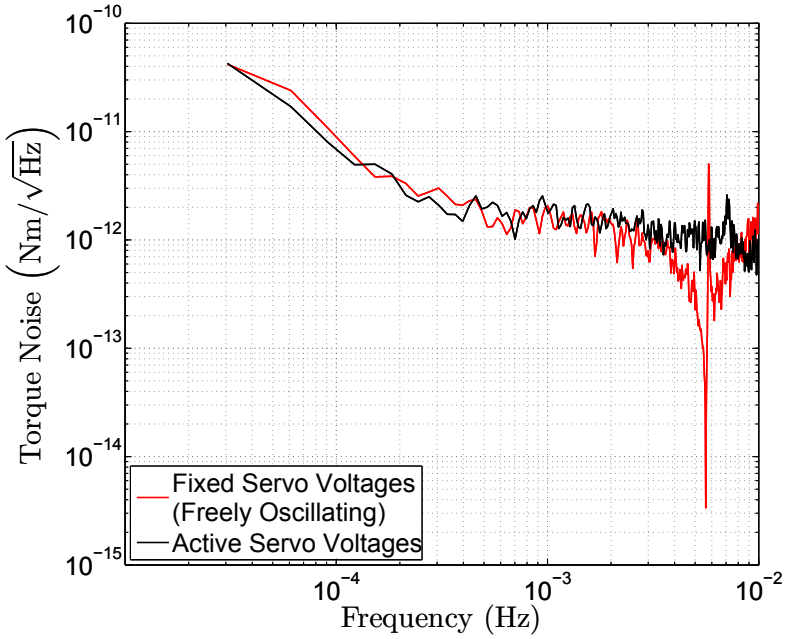

Figure 7. A plot of the torque noise spectra observed while the torsion balance is in free running mode, red, and while under servo control, black. This indicates that the calibration of the instrument under servo control is accurate. The spike in the freely oscillating data (red) at 5.6 mHz is the natural resonance peak of the torsion bob. The spike in the active servo spectrum (black) at 7.1 mHz is the resonance of the bob while it is under servo control. The resonance of the bob under servo control is dependant on the servo parameters.

The full derivation of Eq. 5 and a more detailed account of the torsion balance calibration process can be found in ref. [15].

4. Results

A silica disc was charged under vacuum by pressing it against the copper pad held at a potential of 10 V. The disc was pressed against the pad multiple times in order to deposit a large amount of charge onto the surface. The sample was then moved into position using motorised stages so that the charged surface of the silica sample was facing one of the plates at the ends of the arms of the torsion bob. The silica disc was spaced approximately 18 mm from the plate of the bob. Initially, the bob could

not be servo controlled due to the large DC torque exerted on it by the charge. The bob had to be rotated through an angle of 0.55 rad, or 31.5°, in the x-y plane shown in Figure 1 so that the restoring torque of the fibre would help cancel out the DC torque from the surface charge. Under these conditions, servo control was possible, and the measurement was allowed to take place over the next several days.

Figure 8 shows the noise level of the instrument when a charged sample is near the bob and when there is no charged sample in the vacuum chamber. Figure 8 shows a clear increase in the noise of the instrument when a charged insulator is near the bob of the torsion balance. The noise observed is over three orders of magnitude more than normally observed at some frequencies under optimum operating conditions. This increase in noise can only be due to the decaying electrostatic charges on the silica sample and not merely due to the introduction of an electrostatic stiffness. As a test, electrostatic stiffness was created by applying high DC voltages to the actuator plates while the torsion balance was freely oscillating and no increase in noise was observed.

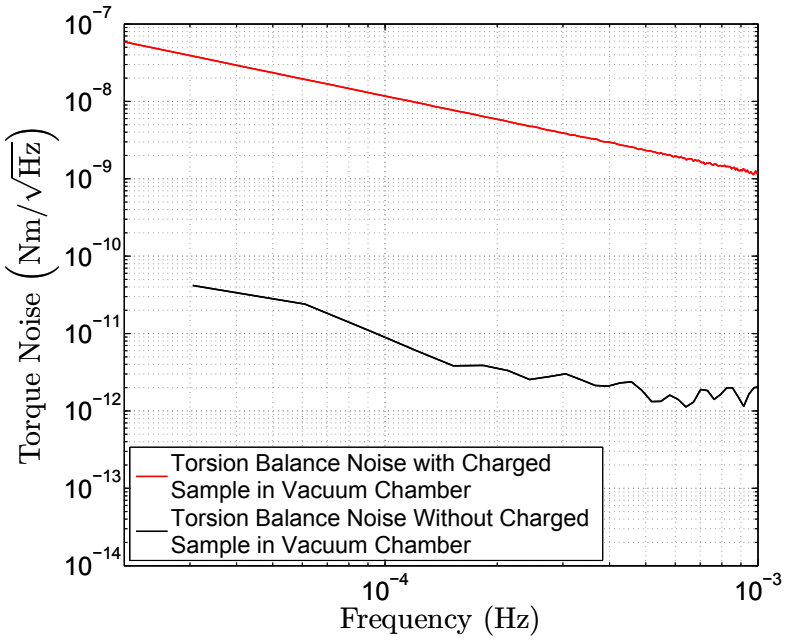

Figure 8. A plot of the torque noise levels of the torsion balance with a charged sample near the bob, red, and without a charged sample near the bob, black.

The charging noise expected from this measurement must be calculated to determine whether the noise observed is consistent with that given by (2). Charging noise is dependent upon the average Coulomb force, or torque in this instance, exerted on the torsion bob and the correlation time of the charge. Therefore, to calculate the charging noise signal that should be expected from this measurement the average DC torque acting on the bob and the correlation time of the charge must be determined.

4.1. Estimating the DC Torque Exerted on the Torsion Bob

The DC Coulomb torque was estimated from the restoring torque acting on the torsion bob. The restoring torque and the Coulomb torque from the surface charge should be equal, but opposite, when the bob is perfectly centered between the sensor and actuator plates. The restoring torque comprises of two components: the restoring torque of the fibre and the torque applied by the servo actuators. The magnitude of the restoring torque of the fibre, Γ_1, can be calculated simply from the angle through which the bob was rotated, ϕ, and the stiffness of the fibre, κ,

$$\Gamma_1 = -\phi\kappa \tag{6}$$

From work carried out in [15] it was found that κ is 6.5×10^{-8} Nm/rad and ϕ is 0.55 rad, as mentioned previously. This gives Γ_1 a value of $(3.58 \pm 0.018) \times 10^{-8}$ Nm. The error is taken as the resulting Poisson error from counting the number of steps taken by the stepper motor to rotate the torsion bob 0.55 rad.

The servo torque that is exerted on the bob by the servo actuators can be calculated using,

$$\Gamma_2 = \frac{1}{2}\frac{\mathrm{d}C}{\mathrm{d}\theta}\left(V_1 - V_2\right)^2 \tag{7}$$

where $\frac{\mathrm{d}C}{\mathrm{d}\theta}$ is the average capacitance gradient between the bob and the two servo plates and V_1 and V_2 are the average servo voltages applied to the servo actuators (which will now be referred to servo actuator 1 and 2) over the course of the measurement. The average capacitance gradient was calculated to be $(1.2 \pm 0.4) \times 10^{-11}$ F/rad from measurements made in ref. [15], the average voltage applied to servo actuator 1 was 11.26 V and the average voltage applied to servo actuator 2 was 14.96 V. This gives Γ_2 a value of $(8.21 \pm 2.74) \times 10^{-11}$ Nm, therefore, the combined restoring torque of Γ_1 and Γ_2 is $(3.57 \pm 0.018) \times 10^{-8}$ Nm.

4.2. Estimating the Charging Noise Correlation Time

Figure 9 shows the decaying Kelvin probe signal that was measured during the experiment. The correlation time, τ_0, of the charge can be obtained from the inverse of the time coefficient in the exponential term of the exponential fit to the data, also shown in Figure 9. τ_0 was measured to be 3.01×10^6 s, or approximately 35 days. τ_0 is affected by the cleanliness of the optic. In order to maximise the charging noise level, the surface of the optic was deliberately touched with an ungloved hand to dirty the optic. This caused τ_0 to significantly decrease.

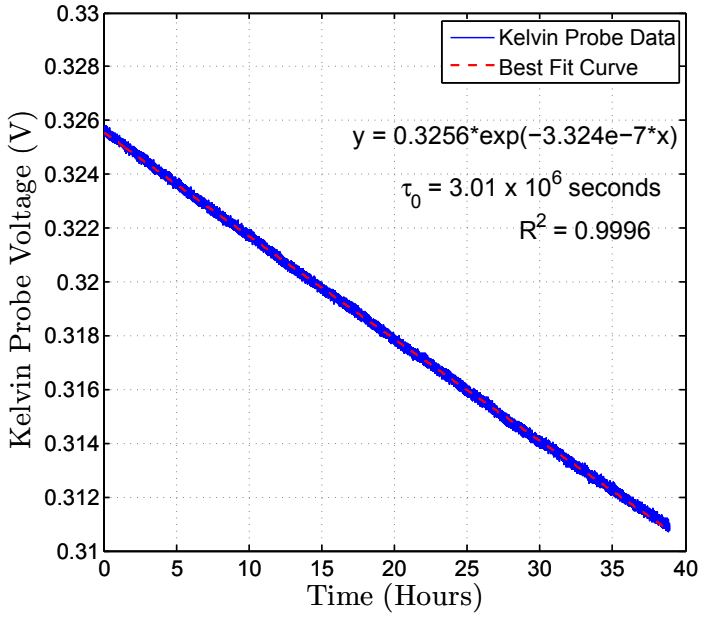

Figure 9. A plot of the decaying Kelvin probe signal measured. The correlation time of the charge, which was determined from an exponential fit to the data, was calculated to be 3.01×10^6 s.

4.3. Comparing the Measured Torsion Balance Noise Level with the Theoretical Charging Noise Level

Determining τ_0 and the average torque, $\langle \Gamma_0 \rangle$, allows the level of charging noise that should be expected in the experiment, using the Weiss theory of charging noise, to

be calculated. The torque noise power spectrum was calculated using,

$$\Gamma^2(f) = \frac{\langle \Gamma_0^2 \rangle}{2\pi\tau_0 \left(\frac{1}{\tau_0^2} + (2\pi f)^2 \right)}. \tag{8}$$

The charging noise level calculated using (8) is shown in Figure 10 along with the observed noise spectrum of the torsion balance measured during the charging noise experiment.

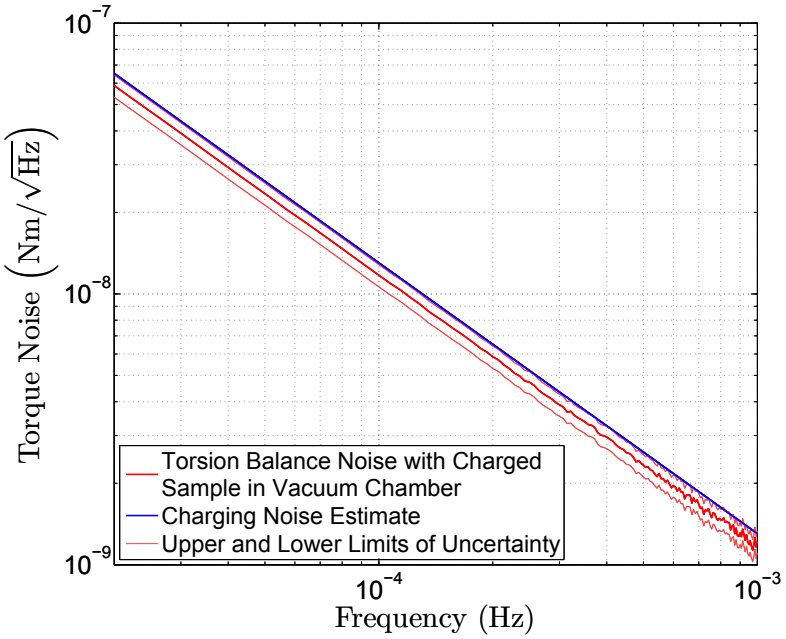

Figure 10. A plot of the observed charging noise spectrum measured with the torsion balance, red, along with the theoretical estimate of the noise level expected from charging noise, blue. The pink lines on the plot indicate the error on the measured charging noise signal. The theoretical charging noise estimate lies on the edge of the upper uncertainty limit.

The theoretical estimate of the charging noise level is less than 1% outside the uncertainty region of the measured charging noise signal. It is possible that the calibration uncertainty has been underestimated due to the fact that the torsion balance is difficult to control under normal operating conditions using the PID control parameters used during the charging measurement, as was required when

calibrating the instrument. Nevertheless, the deviation of the theoretical estimate and the measured charging noise signal is marginal and we are confident that the theory for calculating charging noise is accurate. Another important aspect of this result that proves that the charging noise theory is correct is that the frequency dependance of the measured signal matches that of the theoretical estimate.

5. Conclusion and Future Work

This experiment has successfully measured excess noise due to fluctuating electric charges on a dielectric surface. It has shown that the nature of charging noise can be best described by a Markov process with a single correlation time and has a frequency dependence of f^{-1}, as stated by Weiss [13]. This means that accurate estimates of charging noise can be made for advanced and future gravitational wave detectors which will be extremely useful when planning their construction.

The torsion balance apparatus used in this experiment will soon be upgraded. The main changes to the setup will be that the senors/actuators will be contained in a special housing which will shield them from any noise sources that may be present in the tank and the drive signal will no longer be applied down the torsion fibre like in the setup used for this work. The drive signal will be applied capacitively to the end masses so that the majority of the bob will remain grounded. These efforts will ensure that the new instrument will give better noise performance than the instrument used for this investigation. In the current setup there is no system in place to remove the effects of ground tilt. It is planned that the vacuum tank will sit on a servo controlled stage that will help remove tilt effects. This will allow more accurate measurements of charging noise to be made and future work with the new setup will include measurements on optics with advanced dielectric coatings planned for use in future generation gravitational wave detectors. These measurements will be used in estimations of the charging noise in future detectors.

There are also plans to measure silica samples partly coated with zinc oxide (ZnO). Studies have shown that by adding a small percentage of aluminium into the ZnO coating, the sheet resistivity can be varied by over an order of magnitude [17, 18]. By measuring samples with varying time constants we will be further able to investigate whether the level of charging noise scales with $1/\tau_0$ as predicted by the Weiss theory.

Acknowledgments

The authors are grateful for the financial support provided by Science and Technology Facilities Council (STFC), the Royal Society of Edinburgh (RSE), the Scottish Funding Council (SFC) and the University of Glasgow in the UK. The authors would like to thank the School of Physics and Astronomy workshop at the University of Glasgow for manufacturing the parts for the work presented in this article and Russell Jones and Michael Perreur-Lloyd (University of Glasgow) for useful discussions on engineering the parts for this work. We also thank Dr. Terry Quinn (former head of International Bureau of Weights and Measures), Prof. James Faller (JILA, University of Colorado) and Dr. Bjoern Seitz (University of Glasgow) for fruitful discussions regarding this work. Finally we would like to thank our colleagues in the LSC, the LIGO charging working group and within SUPA for their support and interest in this work.

References

[1] B P Abbott et al. LIGO: The laser interferometer gravitational-wave observatory. *Rep. Prog. Phys.*, 72:076901, 2009.

[2] T Accadia et al. Virgo: a laser interferometer to detect gravitational waves. *J. Instrum.*, 7:P03012, 2012.

[3] H Grote et al. The GEO 600 status. *Class. Quantum Grav.*, 27:084003, 2010.

[4] R Takahashi et al. Status of TAMA300. *Class. Quantum Grav.*, 21(5):S403S408, 2004.

[5] G M Harry et al. Advanced LIGO: the next generation of gravitational wave detectors. *Class. Quantum Grav.*, 27:084006, 2010.

[6] The advanced LIGO team. *Advanced LIGO Reference Design.* Internal LIGO Technical Note M060056-08-M, 2007.

[7] R Amin. *Brief of the May 2006 LIGO Charging Event.* Internal LIGO Technical Note G070572-x0, 2007.

[8] M Hewitson, K Danzmann, H Grote, S Hild, J Hough, H Lück, S Rowan, J R Smith, K A Strain, and B Willke. Charge measurement and mitigation for the main test masses of the GEO 600 gravitational wave observatory. *Class. Quantum Grav.* , 24:6379, 2007.

[9] D Ugolini, R Amin, G M Harry, J Hough, I Martin, V Mitrofanov, et al. Charging issues in LIGO. In *Proceedings of the 30th International Cosmic Ray Conference*, volume 3, pages 1283–1286, 2008.

[10] V P Mitrofanov, L G Prokhorov, and K V Tokmakov. Variation of electric charge on prototype of fused silica test mass of gravitational wave antenna. *Phys. Lett. A*, 300:370–374, 2002.

[11] V P Mitrofanov, L G Prokhorov, K V Tokmakov, and P Willems. Investigation of effects

associated with variation of electric charge on a fused silica test mass. *Class. Quantum Grav.*, 21:S1083–S1089, 2004.

[12] V B Braginsky, O G Ryazhskaya, and S P Vyatchanin. Limitations in quantum measurements resolution created by cosmic rays. *Phys. Lett. A*, 359:86–89, 2006.

[13] R Weiss. *Note on electrostatics in the LIGO suspensions.* Internal LIGO Technical Note T960137-00, 1995.

[14] P Campsie, G D Hammond, J Hough, and S Rowan. *J. Phys.: Conf. Ser.*, 363:012006, 2012.

[15] P Campsie. *Investigations of charging noise in future gravitational wave detectors.* PhD thesis, University of Glasgow, 2013.

[16] P Campsie, L Cunningham, M Hendry, J Hough, S Reid, S Rowan, and G D Hammond. Charge mitigation techniques using glow and corona discharges for advanced gravitational wave detectors. *Class. Quantum Grav.*, 28:215016, 2011.

[17] A S Markosyan, R Bassiri, B Lantz, R Route, R Shimshock, and M M Fejer. *Sheet resistivity and optical absorption of ZnO thin films: an attempt to obtain a conductive dielectric layer.* Internal LIGO Technical Note G1300264, 2013.

[18] J Xu, H Wang, L Yang, M Jiang, s Wei, and T Zhang. Low temperature growth of highly crystallized zno:al films by ultrasonic spray pyrolysis from acetylacetone salt. *Mater. Sci. Eng. B*, 167:182–186, 2010.